

Power of a Remote Hydrogen Bond Donor: Anion Recognition and Structural Consequences Revealed by IR Spectroscopy

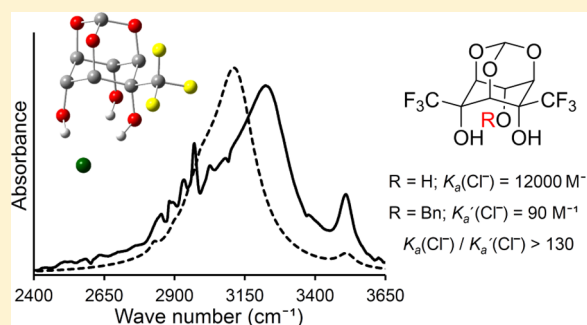
Masoud Samet,[†] Mohammad Danesh-Yazdi,[‡] Alireza Fattahi,[§] and Steven R. Kass^{*,†}

[†]Department of Chemistry, and [‡]St. Anthony Falls Laboratory and Department of Civil Engineering, University of Minnesota, Minneapolis, Minnesota 55455, United States

[§]Department of Chemistry, Sharif University of Technology, Tehran, Iran

S Supporting Information

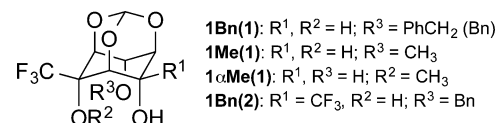
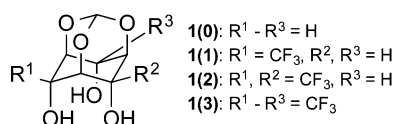
ABSTRACT: Natural and synthetic anion receptors are extensively employed, but the structures of their bound complexes are difficult to determine in the liquid phase. Infrared spectroscopy is used in this work to characterize the solution structures of bound anion receptors for the first time, and surprisingly only two of three hydroxyl groups of the neutral aliphatic triols are found to directly interact with Cl⁻. The binding constants of these triols with zero to three CF₃ groups were measured in a polar environment, and $K_{\text{CD}_3\text{CN}}(\text{Cl}^-) = 1.1 \times 10^6 \text{ M}^{-1}$ for the tris(trifluoromethyl) derivative. This is a remarkably large value, and high selectivity with respect to interfering anions such as Br⁻, NO₃⁻ and NCS⁻ is also displayed. The effects of the third “noninteracting” hydroxyl groups on the structures and binding constants were also explored, and surprisingly they are as large or larger than the OH substituents that hydrogen bond to Cl⁻. That is, a remote hydroxyl group can play a larger role in binding than two OH substituents that directly interact with an anionic center.



INTRODUCTION

Hydrogen bond networks (HBN) are routinely exploited in nature to enable anion transport across nonpolar cellular membrane phospholipid bilayers.^{1–6} One example is the Cl⁻ chloride ion channel which uses a series of NH and OH hydrogen bond donors to bind Cl⁻.⁴ HBN are also employed in synthetic anion receptors containing multiple amides, (thio)ureas, and aryl and aliphatic hydroxyl substituents.^{7–13} For example, a flexible polyol with seven hydroxyl substituents (i.e., (HOCH₂CH₂CH(OH)CH₂)₃COH), was found to bind chloride in acetonitrile with a binding constant of 362 M⁻¹.⁹ The structures of host–guest complexes and bound catalysts of small systems are most commonly determined by X-ray crystallography and gas-phase computations whereas NMR studies have been used and play a large role in biological studies.¹⁴ Both of the former approaches, however, may give different representations of the structures in solution. In this report, IR spectroscopy is used to determine the geometries of anion–receptor complexes for the first time. The binding constants of a series of rigid triols (1(0)–1(3)) and several monoprotected ethers with tetrabutylammonium salts are also reported. The tris(trifluoromethyl) derivative 1(3) is found to be the strongest hydroxyl-based chloride receptor to date and has high selectivity for Cl⁻ over interfering anions such as Br⁻, NO₃⁻, and NCS⁻.¹⁵ A “noninteracting” hydroxyl group is also found to influence the structure of the bound substrate and has as large or a larger influence on the association constants than

two OH substituents that form hydrogen bonds to the anionic guest.



RESULTS AND DISCUSSION

scyllo-Inositol monoorthoformate 1(0) was found to bind chloride ion in acetonitrile with an association constant (K) of 540 M⁻¹. To increase this value, one of the equatorial hydrogens in 1(0) was replaced by an electron-withdrawing CF₃ group. The resulting triol 1(1) has a binding constant of 2800 M⁻¹, which is 5 times larger than for 1(0). It is also ~2 and 20 times bigger than for catechol (1,2-C₆H₄(OH)₂) and resorcinol (1,3-C₆H₄(OH)₂), respectively.¹⁶ Sequential incorporation of a second and third trifluoromethyl group into 1(0) leads to further enhancements of more than 3 orders of

Received: November 20, 2014

Published: December 9, 2014

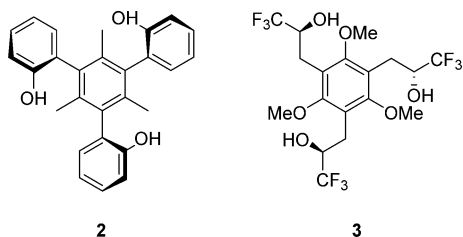
magnitude relative to the unsubstituted triol (Table 1).¹⁷ The association constant for **1(3)** is also 10 and 130 times bigger

Table 1. Measured Binding Constants and Selectivities for **1(0)**–**1(3)**

ion ^{a,b}	K (M ⁻¹) ^c			
	1(0)	1(1)	1(2)	1(3)
Cl ⁻	540	2800	1.2 × 10 ⁴	1.1 × 10 ⁶
Br ⁻	94	190	860	3300
I ⁻			27	110
NO ₃ ⁻		68	120	970
NCS ⁻				270
Cl ⁻ /Br ⁻	5.8	15	14	340
Cl ⁻ /I ⁻			430	1.0 × 10 ⁴
Cl ⁻ /NO ₃ ⁻		42	98	1100
Cl ⁻ /NCS ⁻				4200

^aTetrabutylammonium salts were used in all cases. ^bFor HSO₄⁻, *K* was too small to measure with **1(3)**. ^cEstimated errors are ~20% except for **1(3)** with Cl⁻, which is less certain since NMR determinations are less reliable when *K* ≥ 10⁵ M⁻¹ (ref 17).

than for **2** and **3**, respectively.^{10,11} It is also the largest value reported to date for a noncharged alcohol even though it is an aliphatic alcohol rather than a phenol; the latter species are inherently more acidic and typically have high anion affinities.



Anion recognition and selective binding play a critical role in the development of synthetic ion transporters and sensors.^{15,18} Triol **1(3)** is a preorganized receptor and was found to selectively bind Cl⁻ over common interfering anions such as Br⁻, NO₃⁻, and NCS⁻. Interestingly, the selectivity order follows the gas-phase acidities of the conjugate acids and not the Hofmeister series (i.e., Cl⁻ > NO₃⁻ > Br⁻ > I⁻ > SCN⁻).¹⁹ That is, Δ*G*_{acid}^o HCl (328.1 ± 0.1) < HBr (318.3 ± 0.2) < HNO₃ (317.8 ± 0.2) < HNCS (≤317.6 ± 1.4) < HI (309.3 ± 0.1) < H₂SO₄ (302.3 ± 5.5 kcal mol⁻¹) where HCl is the least acidic of these acids and H₂SO₄ is the strongest one.²⁰ Sterics, electrostatics, and the size of the binding cavity must play a role, too, in the observed selectivities and the magnitudes of the binding constants.

One would expect the chloride anion complexes of triols **1(0)**–**1(3)** to adopt structures with three direct (i.e., primary) OH...Cl⁻ interactions because hydrogen bonds to anionic centers are known to be very stabilizing,²¹ and this is the reported bonding motif for **2** and **3**.^{10,11} Gas-phase B3LYP/6-31+G(d,p) computations were carried out on all four triols and their bound cluster anions, and structures with one to three OH...Cl⁻ interactions were located in all four cases (Figure 1 and Supporting Information). Surprisingly, the most stable conformers were found to have two primary hydrogen bonds and one bifurcated secondary interaction (**a** and **b**). The less stable structures (**c** and **d**) suffer from electron–electron repulsion due to the overlap of the lone pairs of electrons on the oxygen and fluorine atoms whereas this effect is mitigated

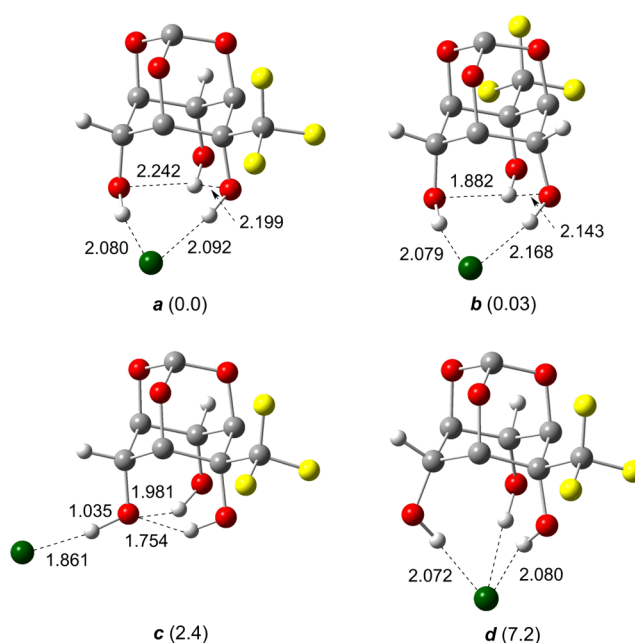


Figure 1. DFT geometries of **1(1)**·Cl⁻ where the bridgehead and apical hydrogens are removed for clarity; parenthetical values are relative energies in kcal mol⁻¹, O–H distances are <1.00 Å unless specified, and **d** has C₃ symmetry.

by the secondary hydrogen bond in **a** and **b**. The least stable species (**d**) also has distorted C–O–H bond angles to accommodate the three OH...Cl⁻ interactions. As for the small differences in the stability between **a** and **b**, this may appear to be surprising since one would expect the OH on the carbon bearing the CF₃ group to be the most acidic site and the better hydrogen bond donor. In **a** this substituent also serves as a hydrogen bond acceptor but the CF₃ group diminishes its capability in this regard. In **b** this OH substituent does not directly interact with the chloride anion and only functions as a hydrogen bond donor. As a result, there is little preference as to which two OH groups are used to hydrogen bond to Cl⁻.

To experimentally probe the structures of the anion–receptor complexes, 10 mM solutions of **1(1)**, **1(3)**, and their tetra-*n*-butylammonium chloride (TBACl) complexes were studied in 10:90 CD₃CN/CCl₄ mixtures by IR spectroscopy.^{22,23} The spectra for both compounds are similar, so only the results for triol **1(1)** are discussed and the data for **1(3)** is given in the Supporting Information (Figure S5 and Table S5). A strong broad OH band at 3436 cm⁻¹ and four weak C–H absorptions at 3029, 2970, 2930, and 2856 cm⁻¹ are observed for **1(1)** (Figure 2). The former feature is ~178 cm⁻¹ lower than the free OH stretch of *cis*-cyclohexane-1,3-diol in CCl₄²⁴ due, at least in large part, to the hydrogen bond-accepting ability of the acetonitrile cosolvent.²⁵ Gas-phase B3LYP/6-31+G(d,p) computations reproduce the experimental spectrum nevertheless, and the predicted bands at 3492, 3024, 2945, and 2915 cm⁻¹ are within 5 to 59 cm⁻¹ of the observed frequencies.

Upon the addition of 1 equiv of TBACl to **1(1)**, two new OH stretching bands appeared at 3513 and 3217 cm⁻¹ (Figure 3). The former feature is due to a relatively free hydroxyl group with a weak hydrogen bond whereas the large 219 cm⁻¹ red shift for the latter band is the result of strong OH...Cl⁻ interactions. A new weak C–H stretch is also observed below 2900 cm⁻¹ at 2882 cm⁻¹ in addition to four little changed bands at 3028, 2973, 2934, and 2853 cm⁻¹. These results

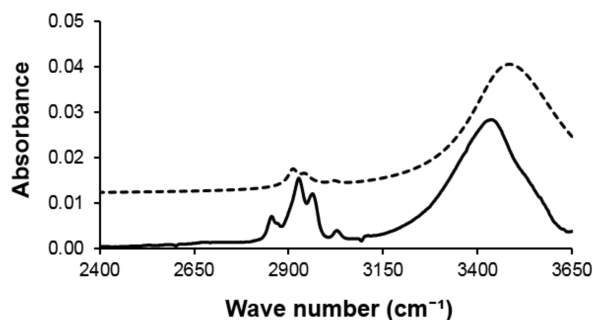


Figure 2. Experimental (solid line) and B3LYP/6-31+G(d,p) calculated (dashed line) IR spectra of **1(1)**. Computed frequencies are scaled by 0.945, and the simulated spectrum was obtained using Lorentzian functions with peak widths at half height ranging from 10 to 100 cm^{-1} .

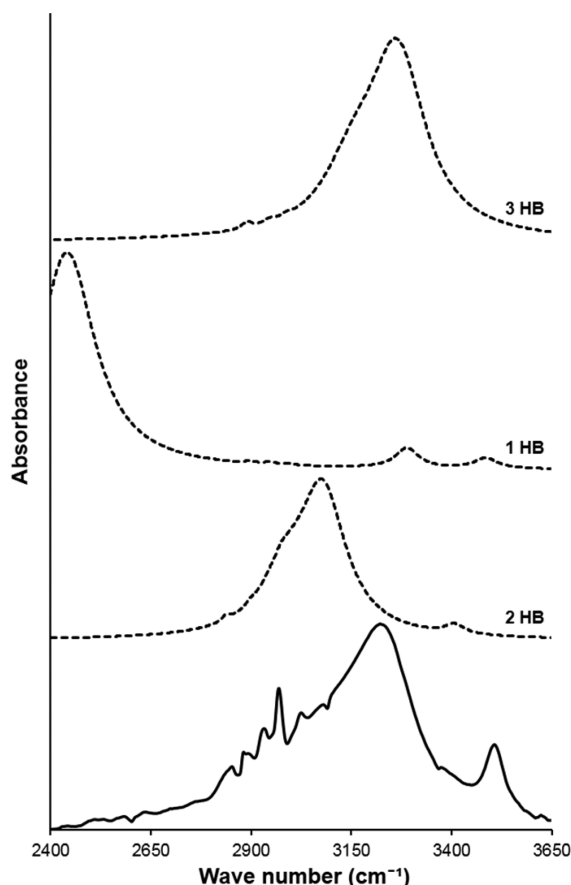


Figure 3. Experimental (solid line) and B3LYP/6-31+G(d,p) computed (dashed lines) IR spectra of **1(1)·Cl⁻**. Computed spectra are for conformers with one to three primary hydrogen bonds (HB) to Cl^- as indicated.

suggest that the major structure of **1(1)·Cl⁻** has two $\text{OH}\cdots\text{Cl}^-$ hydrogen bonds and a weak $\text{OH}\cdots\text{X}$ one, where $\text{X} = \text{OH}$ or NCCD_3 . The alternative structures with one and three primary interactions are inconsistent with the experimental data. That is, the red shift for the $\text{O}-\text{H}$ stretch of the former species should be much larger (e.g., it is 672 cm^{-1} for $(\text{CF}_3)_3\text{COH}\cdots\text{Cl}^-$) and the latter conformer has no weakly bound OH groups. Proton transfer also can be ruled out since Cl^- is a weak base, the $\text{H}-\text{Cl}$ stretch appears at 2833 cm^{-1} in CCl_4 ,²⁶ and its hydrogen bonded complex should be located at even lower frequency.

Computed B3LYP/6-31+G(d,p) IR spectra for the different conformers of **1(1)·Cl⁻** are distinct, and the one with two primary hydrogen bonds is in good accord with experiment as expected (Figure 3).²⁷ The red shift for the structure with one HB is too large, and the species with three HB does not have a free OH band. An expansion of the low frequency $\text{C}-\text{H}$ stretching region due to the equatorial methine hydrogens is also diagnostic when the spectrum is recorded in 30% $\text{CD}_3\text{CN}/70\% \text{CCl}_4$ with Ph_4PCl and is in accord with the two $\text{OH}\cdots\text{Cl}^-$ structure (Figures S7 and S8, Supporting Information). Energetically this species is predicted to be the most stable as well in that the enthalpies at 298 K for the one to three hydrogen bond structures are 2.4, 0.0, and 7.2 kcal mol^{-1} , respectively.

These results suggest that the third hydroxyl group in **1(0)-1(3)** may be relatively unimportant with respect to anion binding and the resulting structure of the bound complex. To address this issue, several monoprotected ethers were prepared and examined. The association constants for the two methyl ethers of **1(1)** (i.e., **1Me(1)** and **1 α Me(1)**) in CD_3CN upon adding TBACl were both found to be 210 M^{-1} . These values correspond to an ~ 15 fold reduction in the binding constants relative to **1(1)**, which indicates that the third hydroxyl group is worth at least as much as one of the other two even though it does not directly interact with the chloride anion. An even larger reduction of 130 fold was found for the benzyl ether of **1(2)** (i.e., **1Bn(2)**) in that $K = 90\text{ M}^{-1}$. Sterics may play a minor role in the diminishment of this association constant but are unlikely to be of major significance since there is essentially no difference in K for **1Me(1)** and **1Bn(1)** which are 210 and 170 M^{-1} , respectively. This indicates that the remote hydroxyl substituent in **1(2)** has a bigger effect on the binding constant than the two OH substituents that hydrogen bond directly to the chloride anion in the bound complex. This finding is in keeping with a similar observation based upon gas-phase photoelectron spectra and computations²⁸ and has obvious implications in biological processes such as binding, catalysis, protein folding, etc.

IR spectra of **1Bn(1)**, **1Bn(2)**, and their TBACl complexes in carbon tetrachloride were recorded to investigate the structures of the bound monoprotected triols (Figures 4, and Figure S9, Supporting Information). Due to the enhanced solubility of these compounds in CCl_4 , CD_3CN was not needed or used as a cosolvent. A strong red-shifted OH absorption at $\leq 3000\text{ cm}^{-1}$ and a weak OH stretch at $\sim 3430\text{ cm}^{-1}$ were observed in both of the bound complexes. The latter features are due to relatively free hydroxyl groups that are slightly red-shifted (i.e., $<100\text{ cm}^{-1}$) due to intramolecular $\text{O}-\text{H}\cdots\text{O}$ interactions, and they indicate that the bound receptors adopt structures with only one hydrogen bond to the chloride anion (Figure 5). This structural change in the two diols relative to their unprotected triols is in accord with computations. That is, B3LYP/6-31+G(d,p) energies of the corresponding methyl ethers favor the structures with one rather than two hydrogen bonds to Cl^- by 5.2 (**1Me(1)**) and 1.5 (**1Me(2)**) kcal mol^{-1} .²⁹ The predicted IR spectra of these species are also in line with this finding, and so the absence of a hydroxyl group that does not directly interact with Cl^- in the bound complexes can nevertheless alter the structures of the bound receptors.

CONCLUSIONS

IR spectroscopy was used to determine the structures of small chloride anion–receptor complexes, and their geometries were

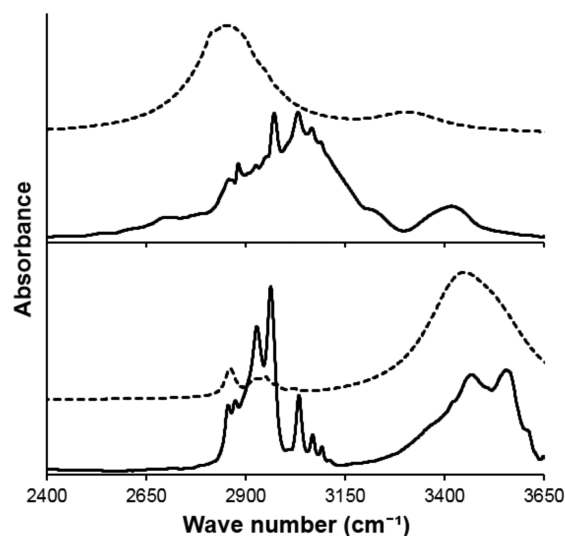


Figure 4. Experimental (solid lines) IR spectra of **1Bn(1)** (bottom) and **1Bn(1)·Cl⁻** (top) and B3LYP/6-31+G(d,p) predictions of the corresponding methyl ethers (dashed lines).

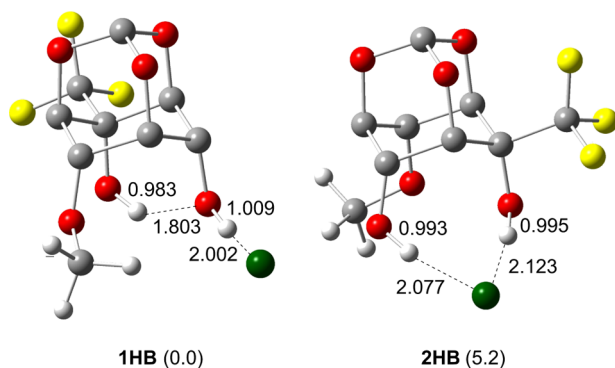


Figure 5. B3LYP/6-31+G(d,p) geometries of **1Me(1)·Cl⁻** as models for the benzyl ether; bridgehead and apical hydrogens are removed for clarity, and parenthetical values are relative energies in kcal mol⁻¹.

found to employ one less hydrogen bond to the ion than was available in the triol (i.e., two rather than three). Protection as an ether of one of the three hydroxyl groups was found, nevertheless, to have as large an effect as one or both of the remaining OH substituents on the chloride anion association constants. It also altered the structures of the bound complexes by eliminating one of the OH...Cl⁻ hydrogen bonds. These results are accounted for by the presence (or absence) of secondary OH...OH hydrogen bond interactions which enable a remote hydroxyl group to play a large structural and energetic role in binding. This has readily apparent implications in numerous biological processes as well as site-directed mutagenesis studies. It is worth noting, too, that triol **1(3)** is found to be a strong and selective binder of Cl⁻ in a polar environment.

EXPERIMENTAL SECTION

General. Triols **1(0)–1(3)** were synthesized as previously reported.²⁸ Acetonitrile-*d*₃ was stored over activated 3 Å molecular sieves for several days, tetrabutylammonium chloride and tetraphenylphosphonium chloride (Ph₄PCl) were stored in a desiccator containing phosphorus pentoxide, and Dess–Martin periodinane (DMP) was prepared according to previously reported procedures.³⁰ Glassware, vials, NMR tubes, and microsyringes were dried in ovens

and allowed to cool under a stream of dry nitrogen or argon. THF was dried by refluxing it over sodium metal under an argon atmosphere using benzophenone as an indicator and subsequently was distilled. Hydrogenation reactions were carried out in a 600 mL stainless steel reactor. TLC analyses were performed on precoated (250 mm) silica gel 60 Å pore size F-254 plates and were visualized by staining with KMnO₄ or a hand-held UV lamp. Medium pressure liquid chromatography (MPLC) was carried out with a commercial instrument in which the samples were dissolved in a minimal amount of CH₂Cl₂ and syringed on to a silica gel (Premium R_f Silica Gel, 60A, 40–75 μm) column. Reported melting points (mp) are uncorrected. Proton, ¹³C, and ¹⁹F NMR spectra were obtained with 300 and 500 MHz spectrometers, and the chemical shifts are reported in ppm and were referenced to the residual solvent as follows: CHCl₃ = 7.27 δ (¹H), 77.0 δ (¹³C); CHD₂CN = 1.94 δ (¹H), 1.39 δ (¹³C). For the ¹⁹F spectra, CF₃CO₂H was used as an external calibrant and assigned a value of -78.5 δ. IR spectra of neat samples were recorded with an ATR source while the solution studies are described below. ESI-TOF mass spectra were obtained using methanolic solutions, and PEG was employed as an internal standard for acquiring high resolution data.

1-Trifluoromethyl-1-methoxy scyllo-Inositol Monoorthoformate (1αMe(1)). 1-Trifluoromethyl-3,5-dibenzyloxy scyllo-inositol monoorthoformate²⁸ (0.850 g, 1.90 mmol) was dissolved in 20 mL of dry THF in a 100 mL round-bottomed flask under argon. This solution was stirred and cooled down to 0 °C, and 0.150 g (3.80 mmol) of a 60% dispersion of NaH in mineral oil was added in several portions. After 30 min, CH₃I (1.06 mL, 2.42 g, 17.1 mmol) was slowly syringed into the flask and the reaction mixture was allowed to warm to room temperature overnight. It was quenched by careful addition of 10 mL of a saturated aqueous solution of NH₄Cl, and the organic layer was separated. Two 20 mL portions of diethyl ether were used to extract the aqueous phase, and the combined organic material was washed with 10 mL of brine. The resulting solution was dried over Na₂SO₄ and concentrated under reduced pressure to afford an oily residue that was purified by MPLC (2/98 to 35/65 EtOAc/hexanes) to give 0.300 g (35%) of 1-trifluoromethyl-1-methoxy-3,5-dibenzyloxy scyllo-inositol monoorthoformate as a white gummy compound (R_f = 0.45 in 14/86 EtOAc/hexanes). Its ¹⁹F NMR showed a new signal at -74.1 ppm and a small residual absorption at -82.0 for the starting material, but an OH stretch was not observed in its IR spectrum. This intermediate compound was consequently taken on without further purification.

1-Trifluoromethyl-1-methoxy-3,5-dibenzyloxy scyllo-inositol monoorthoformate (0.200 g, 0.442 mmol) was dissolved in 6.0 mL of dry THF in a 25 mL round-bottomed flask. Pearlman's catalyst (20% Pd(OH)₂/C, 0.0667 g) was added, and the flask was placed in a hydrogenation apparatus where it was magnetically stirred. The reactor was evacuated and then filled with hydrogen to a pressure of 250 psi three times in succession followed by a 24 h reaction period. Diethyl ether (10 mL) was added to the reaction flask after venting the system, and the resulting solution was filtered through a small plug of silica gel which was subsequently rinsed with 20 mL of diethyl ether. The combined organic material was concentrated under reduced pressure to afford an oily residue and purification by MPLC (10/90 EtOAc/hexanes to neat EtOAc) gave 0.115 g (96%) of **1αMe(1)** as a white solid (R_f = 0.19 in 1/1 EtOAc/hexanes, mp = 167–170 °C) that turned light brown at 165 °C. ¹H NMR (500 MHz, CD₃CN) δ 5.50 (s, 1H), 4.62 (m, 2H), 4.49–4.41 (m, 2H), 4.21 (m, 1H), 4.00 (d, J = 8.8 Hz, 2H), 3.46 (q, J = 2.0 Hz, 3H). ¹³C NMR (125 MHz, CD₃CN) δ 125.8 (q, J = 291 Hz), 102.7, 74.5 (q, J = 25.3 Hz), 71.9, 69.3, 68.4, 54.7 (q, J = 1.8 Hz). ¹⁹F (282 MHz, CD₃CN) δ -73.5. IR (ATR source) 3494, 3370, 3029, 3011, 2993, 2961, 2920, 2855 cm⁻¹. HRMS-ESI: calcd for C₉H₁₀F₃O₆⁻ (M - H)⁻ 271.0435, found 271.0426.

1-Trifluoromethyl-3-benzyloxy scyllo-Inositol Monoorthoformate (1Bn(1)). 5-Trifluoromethyl-5-trimethylsilyloxy-3-benzyloxy scyllo-inositol monoorthoformate²⁸ (1.00 g, 2.38 mmol) was dissolved in 10 mL of dry THF and stirred in a round-bottomed flask under argon. A 1.0 M TBAF solution in THF (7.2 mL) was added in one portion, and after 45 min the resulting light brown mixture was concentrated under reduced pressure. The resulting material was diluted with 50 mL of diethyl ether and passed through a plug of silica gel which was

subsequently rinsed with 100 mL of diethyl ether. Concentration of the combined solutions under reduced pressure and purification by MPLC (1/9 EtOAc/hexanes to neat EtOAc) afforded 0.790 g (96%) of **1Bn(1)** as a white solid ($R_f = 0.38$ in 1/1 EtOAc/hexanes, mp = 115–117 °C). ^1H NMR (500 MHz, CDCl_3) δ 7.42–7.31 (m, 5H), 5.52 (s, 1H), 4.76 (d, $J = 11.3$ Hz, 1H), 4.69 (d, $J = 11.3$ Hz, 1H), 4.63 (m, 1H), 4.56 (s, 1H), 4.51 (m, 4H), 3.27 (d, $J = 8.3$ Hz, 1H). ^{13}C NMR (125 MHz, CDCl_3) δ 135.8, 128.9, 128.8, 128.2, 123.9 (q, $J = 28.4$ Hz), 101.8, 73.7, 72.6, 69.6 (q, $J = 28.9$ Hz), 68.9, 68.5, 67.9, 67.0. ^{19}F NMR (471 MHz, CDCl_3) δ -82.2. IR (ATR source) 3434, 3329, 3096, 3068, 3029, 2975, 2943, 2880 cm^{-1} . HRMS-ESI: calcd for $\text{C}_{15}\text{H}_{14}\text{F}_3\text{O}_6^-$ ($\text{M} - \text{H}$) $^-$ 347.0748, found 347.0774.

1-Trifluoromethyl-5-methoxy scyllo-Inositol Monoorthoformate (1Me(1)). 3-Benzoyloxy-5-methoxy *myo*-inositol monoorthoformate³¹ (0.89 g, 3.02 mmol) was dissolved in 25 mL of dry CH_2Cl_2 in a 100 mL round-bottomed flask under argon. Dess–Martin periodinane (1.54 g, 3.60 mmol) was added, and the reaction mixture was stirred overnight. Removal of the solvent afforded a residue that was diluted with 30 mL of diethyl ether and an equal volume of an aqueous solution consisting of 10% $\text{Na}_2\text{S}_2\text{O}_3$ (15 mL) and 5% NaHCO_3 (15 mL). The resulting slurry was vigorously stirred for 15 min, and then the organic layer was separated, dried over Na_2SO_4 , and concentrated under vacuum to afford 0.84 g (95%) of a viscous yellow oil. This oxidation product showed carbonyl and OH bands in its IR spectrum at 1763 and 3464 cm^{-1} , respectively and was carried on without further purification.

A 25 mL round-bottomed flask was filled with 0.84 g (2.87 mmol) of the crude ketone, 2.55 mL (2.45 g, 17.2 mmol) of TMSCF_3 , and 10 mL of anhydrous THF under an argon atmosphere at 0 °C. A 1.0 M tetrabutylammonium fluoride solution in THF (0.10 mL) was slowly added with stirring, and the resulting mixture was allowed to warm to room temperature overnight. Concentration of this material under reduced pressure afforded an oily residue that was diluted with 10 mL of dry THF. More TBAF (2.90 mL) was added, and the resulting solution was stirred for 1 h. Evaporation of the volatile materials under reduced pressure afforded a residue that was purified by MPLC (1/19 to 1/1 EtOAc/hexanes) to give 0.10 g (10%) of the desired trifluoromethyl-substituted alcohol as a light yellow oil ($R_f = 0.35$ in 1/3 EtOAc/hexanes). ^1H NMR (500 MHz, CDCl_3) δ 7.35 (m, 5H), 5.53 (s, 1H), 5.31 (s, 1H), 4.71 (d, $J = 11.3$ Hz, 1H), 4.68 (d, $J = 11.3$ Hz, 1H), 4.59 (m, 2H), 4.55 (m, 1H), 4.47 (m, 1H), 4.31 (m, 1H), 3.51 (s, 3H). ^{19}F NMR (282 MHz, CDCl_3) δ -81.9. IR (ATR) 3435 cm^{-1} (broad OH band).

The alcohol intermediate (0.10 g, 0.28 mmol) was dissolved in 2 mL of THF in a 10 mL round-bottomed flask. Pearlman's catalyst (33 mg) was added to the reaction mixture, and the flask was placed in a Parr hydrogenation apparatus where it was evacuated and filled with hydrogen to a pressure of 500 psi three times in succession. After 24 h, the system was vented, 5 mL of diethyl ether was added, and the resulting solution was filtered through a small plug of silica gel which was subsequently rinsed with 10 mL of diethyl ether. Concentration of the combined organic material under reduced pressure gave a light yellow solid which was partially dissolved in hot CHCl_3 and allowed to cool to give 60 mg (79%) of **1Me(1)** as a white solid (mp = 88–91 °C). ^1H NMR (500 MHz, CD_3CN) δ 5.51 (s, 1H), 5.26 (s, 1H), 4.55 (m, 2H), 4.47 (m, 1H), 4.38 (m, 1H), 4.26 (m, 1H), 4.16 (d, $J = 6.1$ Hz, 1H), 3.46 (s, 3H). ^{13}C NMR (125 MHz, CD_3CN) δ 125.6 (q, $J = 28.4$ Hz), 102.7, 76.74, 76.73, 70.6 (q, $J = 27.1$ Hz), 69.7, 68.2, 68.1, 58.2. ^{19}F NMR (471 MHz, CD_3CN) δ -81.2. IR (ATR source) 3288, 3062, 3000, 2967, 2947, 2914, 2849 cm^{-1} . HRMS-ESI: calcd for $\text{C}_9\text{H}_{10}\text{F}_3\text{O}_6^-$ ($\text{M} - \text{H}$) $^-$ 271.0435, found 271.0444.

Binding Measurements. Anion affinities were measured in acetonitrile- d_3 at constant and nonaggregating concentrations of **1(1)–1(3)** (i.e., <0.60 mM). These host solutions were titrated with a mixture of the TBAX salt and the alcohol of interest in oven-dried NMR tubes, and changes in the equatorial methine hydrogens chemical shifts were followed except for **1(3)** where the bridgehead hydrogen was monitored. Nonlinear 1:1 fits of the data with the Solver add-on for Excel were carried out to obtain the binding constants (K (M^{-1})).³² Representative tetrabutylammonium chloride titration

results and binding isotherms for **1(0)–1(3)** are provided in Tables S1–S4 and Figures S1–S4, Supporting Information.

IR Studies. Background corrected IR spectra of receptor solutions and their 1:1 TBACl complexes were recorded in NaCl cells with 0.10 and 1.0 mm fixed path lengths. Compounds **1Bn(1)** (4.8 mM) and **1Bn(2)** (6.0 mM) were examined in CCl_4 , whereas 10 mM 10% $\text{CD}_3\text{CN}/90\%$ CCl_4 solutions were used for **1(1)** and **1(3)**. Computed B3LYP/6-31+G(d,p) frequencies were fit with Lorentzian functions, and the resulting intensities at each wavelength n in the spectral window are given by $I(n) = aI_0/(1 + \{(n - bn_0)^2/2S^2\})$, where a , b , n_0 , I_0 , and S are the intensity correction parameter, frequency scaling factor, computed frequency and intensity, and peak width at half height, respectively. To minimize the average least-squares error for the summation of the fitted curves to the experimental spectrum, a wide range of feasible values for the peak widths spanning from 10–100 cm^{-1} were examined by a Monte Carlo approach to find the optimum value using MATLAB. Different scaling factors were also examined, and a value of 0.945 was adopted in this work.

Computations. Full geometry optimizations and subsequent vibrational frequency determinations were carried out at the Minnesota Supercomputer Institute for Advanced Computational Research with Gaussian 09.³³ The Becke three-parameter hybrid exchange and Lee–Yang–Parr correlation density functional (B3LYP) was used in conjunction with the 6-31+G(d,p) basis set.^{34,35} Zero-point energies (zpe) and thermal corrections to the 298 K enthalpies (tc) were obtained from unscaled vibrational frequencies. The resulting geometries and energies are given in ref 16 or are provided in Table S6, Supporting Information.

■ ASSOCIATED CONTENT

📄 Supporting Information

Binding determination data, IR, ^1H and ^{13}C NMR spectra, and computed geometries and energies are provided as is the complete citation to ref 33. This material is available free of charge via the Internet at <http://pubs.acs.org>.

■ AUTHOR INFORMATION

✉ Corresponding Author

*E-mail: kass@umn.edu.

Notes

The authors declare no competing financial interests.

■ ACKNOWLEDGMENTS

We thank Ms. Fatemeh Khodaei Kalaki for her assistance in obtaining the early IR spectra. Generous support from the National Science Foundation, Petroleum Research Fund, as administered by the American Chemical Society, and the Minnesota Supercomputer Institute for Advanced Computational Research are gratefully acknowledged.

■ REFERENCES

- (1) Dutzler, R.; Campbell, E. B.; Cadene, M.; Chait, B. T.; MacKinnon, R. *Nature* **2002**, *415*, 287–294.
- (2) Koropatkin, N. M.; Pakrasi, H. B.; Smith, T. J. *J. Proc. Natl. Acad. Sci. U. S. A.* **2006**, *103*, 9820–9825.
- (3) Luecke, H.; Quioco, F. A. *Nature* **347** **1990**, *347*, 402–406.
- (4) Miller, C. *Nature* **2006**, *440*, 484–489.
- (5) Omata, T. *Plant Cell Physiol.* **1995**, *36*, 207–213.
- (6) Pflugrath, J. W.; Quioco, F. A. *Nature* **1985**, *314*, 257–260.
- (7) Ayling, A. J.; Pérez-Payán, M. N.; Davis, A. P. *J. Am. Chem. Soc.* **2001**, *123*, 12716–12717.
- (8) Winstanley, K. J.; Sayer, A. M.; Smith, D. K. *Org. Biomol. Chem.* **2006**, *4*, 1760–1767.
- (9) Shokri, A.; Schmidt, J.; Wang, X.-B.; Kass, S. R. *J. Am. Chem. Soc.* **2012**, *134*, 16944–16947.

- (10) Beletskiy, E. V.; Schmidt, J.; Wang, X.-B.; Kass, S. R. *J. Am. Chem. Soc.* **2012**, *134*, 18534–18537.
- (11) Shokri, A.; Deng, S. H. M.; Wang, X.-B.; Kass, S. R. *Org. Chem. Front.* **2014**, *1*, 54–61.
- (12) Santacroce, P. V.; Davis, J. T.; Light, M. E.; Gale, P. A.; Iglesias-Sánchez, J. C.; Prados, P.; Quesada, R. *J. Am. Chem. Soc.* **2007**, *129*, 1886–1887.
- (13) Shokri, A.; Wang, X.-B.; Kass, S. R. *J. Am. Chem. Soc.* **2013**, *135*, 9525–9530.
- (14) (a) Wüthrich, K. *J. Biol. Chem.* **1990**, *265*, 22059–22062.
(b) Opella, S. J.; Marassi, F. M. *Chem. Rev.* **2004**, *104*, 3587–3606.
- (15) Buhlmann, P.; Pretsch, E.; Bakker, E. *Chem. Rev.* **1998**, *98*, 1593–1687.
- (16) Smith, D. K. *Org. Biomol. Chem.* **2003**, *1*, 3874–3877.
- (17) Chial, K.; Stelzig, S. H.; Gropeanu, R.; Weil, T.; Klapper, M.; Müllen, K. *Macromolecules* **2009**, *42*, 7545–7552.
- (18) Hay, B. P.; Firman, T. K.; Moyer, B. A. *J. Am. Chem. Soc.* **2005**, *127*, 1810–1819.
- (19) Merenbloom, S. I.; Flick, T. G.; Daly, M. P.; Williams, E. R. *J. Am. Soc. Mass Spectrom.* **2011**, *22*, 1978–1990.
- (20) Bartmess, J. E. *NIST Chemistry WebBook*; NIST Standard Reference Database Number 6; Mallard, W. G., Lustrum, P. J., Eds.; National Institute of Standards and Technology: Gaithersburg, MD (<http://webbook.nist.gov>).
- (21) Shokri, A.; Schmidt, J.; Wang, X.-B.; Kass, S. R. *J. Am. Chem. Soc.* **2011**, *134*, 2094–2099.
- (22) For previous studies using IR spectroscopy to probe anion binding in solution, see: (a) Allerhand, A.; Schleyer, P. v. R. *J. Am. Chem. Soc.* **1963**, *85*, 1233–1237. (b) Kavallieratos, K.; Bertao, C. M.; Crabtree, R. H. *J. Org. Chem.* **1999**, *64*, 1675–1683.
- (23) For a review on gas-phase IR studies that addresses anion-bound complexes, see: Eyler, J. R. *Mass Spectrom. Rev.* **2009**, *28*, 448–467.
- (24) Kuhn, L. P. *J. Am. Chem. Soc.* **1952**, *74*, 2492–2499.
- (25) Vedernikova, E. V.; Gafurov, M. M.; Ataev, M. B. *Russ. Phys. J.* **2011**, *53*, 843–848.
- (26) Leberknight, C. E.; Ord, J. A. *Phys. Rev.* **1937**, *51*, 430–433.
- (27) The predicted spectra for conformers **a** and **b** in Figure 1 are similar, and while the computed spectrum shown in Figure 3 is for **a**, that for **b** (see Figure S6) also provides a good fit to the data and there is no basis to prefer one structure over the other at this time.
- (28) Samet, M.; Wang, X.-B.; Kass, S. R. *J. Phys. Chem. A* **2014**, *118*, 5989–5993.
- (29) The alternate 1 HB structure of **1Me(1)-Cl⁻** is 3.8 kcal mol⁻¹ less stable. This is due to the hydroxyl group on the carbon bearing the trifluoromethyl substituent being a hydrogen bond acceptor and lone pair–lone pair electron repulsion between the chloride anion and one of the fluorines on the CF₃ group.
- (30) (a) Boeckman, R. K., Jr.; Shao, P.; Mullins, J. J. *Org. Synth.* **2000**, *77*, 141–152. (b) Frigerio, M.; Santagostino, M.; Sputore, S. *J. Org. Chem.* **1999**, *64*, 4537–4538.
- (31) Krief, A.; Dumont, W.; Billen, D.; Letesson, J.-J.; Lestrade, P.; Murphyc, P. J.; Lacroix, D. *Tetrahedron Lett.* **2004**, *45*, 1461–1463.
- (32) Connors, K. A. *Binding Constants: The Measurement of Molecular Complex Stability*; Wiley-Interscience: New York, 1987; pp 432.
- (33) Frisch, M. J.; Trucks, G. W.; Schlegel, H. B.; Scuseria, G. E.; Robb, M. A., et al. *Gaussian 09*, Gaussian, Inc., Wallingford, CT, 2009.
- (34) Becke, A. D. *J. Chem. Phys.* **1993**, *98*, 5648–5652.
- (35) Lee, C.; Yang, W.; Parr, R. G. *Phys. Rev. B* **1988**, *37*, 785–789.